Article

Two Potential Ways of Vanadium Extraction from Thin Film Steelmaking Slags

Tetiana Shyrokykh [1,2,*], Lukas Neubert [2], Olena Volkova [2] and Seetharaman Sridhar [1]

[1] School for Engineering of Matter, Transport and Energy, Arizona State University, Tempe, AZ 85287, USA
[2] Institute of Iron and Steel Technology, Technische Universität Bergakademie Freiberg, 09599 Freiberg, Germany; lukas.neubert@iest.tu-freiberg.de (L.N.)
[*] Correspondence: tetiana.shyrokykh@asu.edu

Abstract: During the steelmaking process, a great amount of slag is generated as a by-product. Vanadium-bearing steelmaking slags are classified as hazardous and require special handling and storage due to the toxicity of vanadium pentoxides. At the same time, such slags are valuable sources for the recovery of vanadium. The present work reviews the investigations on vanadium recovery from CaO-SiO_2-FeO-V_2O_5 thin film slags under the neutral and oxidizing conditions in the temperature range 1653 K to 1693 K (1380 °C to 1420 °C) using Single Hot Thermocouple Technique (SHTT). The slag samples were analyzed by SEM/EDX. The results indicated that vanadium pentoxide evaporation can be up to 17.73% under an oxidizing atmosphere, while spinel formation under an argon atmosphere was detected in the conditions of thin film slags.

Keywords: vanadium pentoxide; recycling; Single Hot Thermocouple Technique; evaporation; spinel formation

1. Introduction

The conversion of existing linear economics to more a circular one, where the value of resources and materials is maintained for as long as possible and the waste generation is minimized, is important for developing a resource-efficient, sustainable and competitive economy.

Significant amounts of by-products are generated every year all over the world during the steel production process. In general, the manufacture of one metric ton of steel yields between 200 kg (for electric arc furnace) and 400 kg (for blast furnace and basic oxygen furnace) of by-products, such as slag, dust, and sludge [1]. Slag is the main by-product of the steelmaking industry. Apart from the main slagging components (e.g., CaO, SiO_2, Al_2O_3, MgO, etc.), a significant amount of alloying elements appears in the slag (Mn, V, Cr, etc.) in oxidized form causing problems in further utilization of such slags, e.g., in civil engineering. Vanadium-containing slag is among them. It is classified as toxic material [2] due to its potential environmental and health risks. As a by-product of steelmaking, it requires proper management since it requires special handling, storage, and partial landfill. The utilization of vanadium-containing slag can contribute to the transition towards a more circular economy by preventing landfill waste and preserving natural resources, hence also reducing greenhouse gas (GHG) emissions. Moreover, vanadium is a very valuable alloying component of steelmaking, which significantly improves the quality of the final steel products by reducing the steel grain size, thus improving the wear resistance of the final products. Vanadium is also a key component in non-ferrous alloys, e.g., in Ti-6%Al-4%V which is used for the aircraft industry where lightness and high strength are important, and in additive manufacturing powder and for the production of body implants and prosthetics.

Existing technologies to remove vanadium from the slags—direct acid leaching [3–8], sodium salt roasting [9–11], hot slag reduction [12], and bioleaching [13]—have their

advantages and limitations, and the choice of technology depends on different factors including economic and environmental considerations. The sodium roasting-water leaching method is the most commonly used one to extract vanadium from V-bearing slags [14], but at the same time it presents several environmental challenges, including (1) decomposition of sodium salts creates harmful gases such as HCl, Cl_2, SO_2, SO_3, and CO_2 [15], which pollute the air and damage equipment used in the extraction process; (2) wastewater generated during extraction has high concentrations of sodium and ammonium sulfates, making it difficult to reuse [16]; (3) the resulting leaching residues have a high sodium content, making them unusable and unsuitable for recycling because sodium corrodes the lining of blast furnaces and converters; (4) water leaching residue contains 1–3% of V_2O_5 which is currently turning into waste [17]. This results in the accumulation of leaching residues, which consume valuable land resources [18]. Bioleaching is based on the capability of certain microorganisms to transform solid compounds into extractable, water-soluble forms. However, it also has drawbacks including (1) bacterial leaching occurs very slowly (often taking several months) and cannot be quickly halted once initiated, unlike other methods; (2) the heat produced during the dissolving process can be fatal to the microorganisms involved; (3) large open spaces for treatment procedures are required; (4) high risk of contamination.

One of the ways to extract the compound from the liquid mix could be vaporization. It is well known that some slag constituents have higher vapor pressure in the molten state than the rest of the slag [19]. For example, much attention was dedicated to CaF_2 evaporation from the slags [20–22]. Some pioneering works on CrO_3 [23,24] and V_2O_5 [25,26] volatilization from steelmaking slags are relatively well addressed in the literature. These oxides constitute a serious health hazard, and their evaporation should be controlled in the areas of molten steel tapping. Vanadium pentoxide evaporation leads to a vanadium loss during steel alloying with V_2O_5 [27]. Additionally, a vaporization study [28] for bulk synthetic slags with 6–8% V_2O_5 performed by two of the present authors should be mentioned. A combination of oxidation blowing and vacuum extirpation was applied to the 22 g of molten slag samples. After 60 min oxygen treatment time more than 77% of V_2O_5 was evaporated.

In this context, the present study aims to investigate the potential of extraction of vanadium from steelmaking slags through pyrometallurgical processes. The results of this study could provide valuable insights into the development of sustainable practices for the management of vanadium-containing slag and the recovery of critical metals from industrial by-products.

2. Thermodynamic Considerations

Figure 1 displays the stability of vanadium oxides under various oxygen partial pressures and temperatures. The results indicate that V_2O_5 remains stable across the entire temperature range under oxygen partial pressures equivalent to atmospheric conditions. Consequently, vanadium metal and lower vanadium oxides tend to oxidize to V_2O_5 upon exposure to air, even if the process is gradual. Moreover, the lower oxides of vanadium exhibit stability with increasing temperature and decreasing oxygen partial pressure.
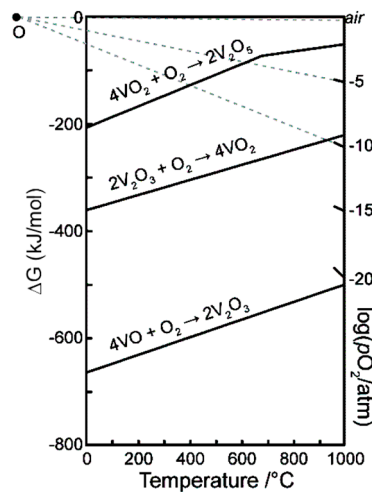
Figure 1. Ellingham diagram for vanadium oxides. Dashed lines show the oxides stability at $P_{O_2} = 0.21$ (air), 10^{-5}, 10^{-10} atm [29,30].

The phase stability diagram of the VO_x system was assessed utilizing FactSage [31], and the outcomes are illustrated in Figure 2. It can be seen from the diagram that V_2O_3 can remain solid at low oxygen pressures while VO_2 is mainly in a liquid state. V_2O_5 is the stable phase under elevated oxygen pressures.
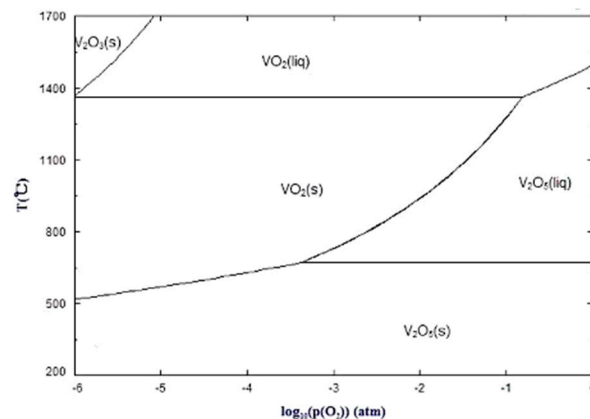

Figure 2. Phase stability diagram of VO_x.

The vapor pressure of vanadium pentoxide as a function of temperature (Figure 3) was calculated using the numerical-value equation given by Kubaschewski and Alcock [32]:

$$\log P = \frac{-7100}{T} + 5.05 \tag{1}$$

where P is vapor pressure in mmHg and T is the temperature in Kelvin.

Considering the relatively low melting point of V_2O_5 equal to 690 °C, one can assume that its vapor pressure would be elevated at temperatures above 1100 °C. Consequently, some vanadium most probably is lost as pentoxide vapor even during the salt roasting process. A study conducted in 2012 [33] examined the evaporation of pure V_2O_5 under various atmospheres at temperatures ranging from 1450–1600 °C using thermogravimetry analysis (TGA). The results (Figure 4) showed that when exposed to a pure oxygen atmosphere (with a flow rate of 400 NmL/min), around 28% of a 100 mg sample could evaporate in 1 h 1600 °C, and in ca., 6 h nearly all of the sample was evaporated. In the air atmosphere vanadium pentoxide evaporation rate was considerably slower—it volatilized only on ca 80% after about 7 h. In the neutral (CO_2) atmosphere ca 35% was evaporated in almost 7 h.
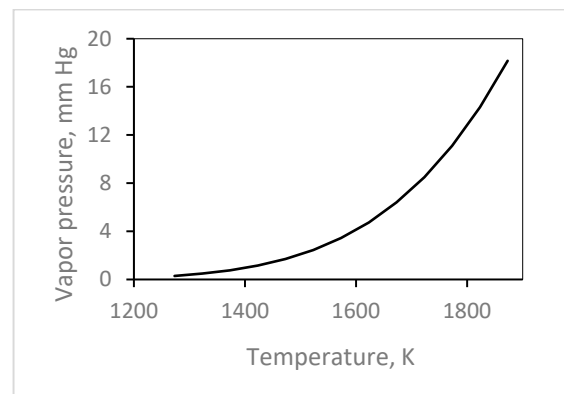
Figure 3. Vapor pressure of V_2O_5 in equilibrium with liquid V_2O_5 as a function of temperature.
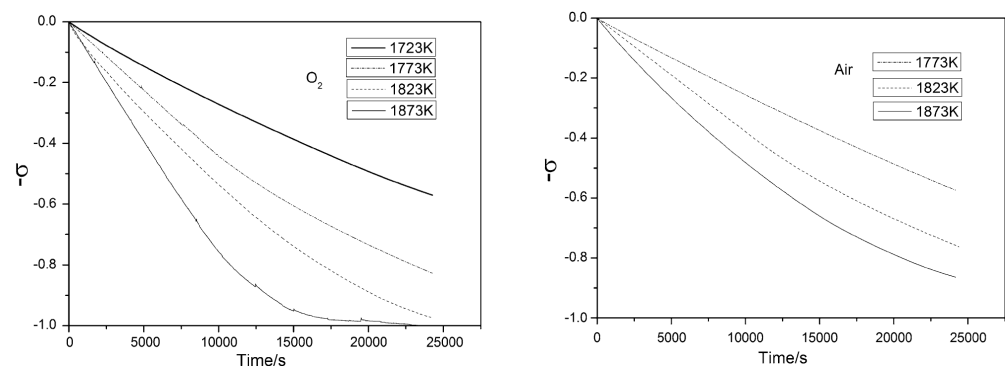

Figure 4. Dimensionless mass loss of V_2O_5 in oxygen and air atmosphere as a function of time and temperature [33].

Wang et al. [27] studied the volatilization of pure V_2O_5 and its mixes in an argon atmosphere and reported a 4.34% mass loss for pure vanadium pentoxide after 10 min at 1600 °C.

In the liquid slag, vanadium can exist in two oxidation states: V^{3+} and V^{4+} [34]. At low oxygen levels, trivalent vanadium is the dominant form in the slag. To evaporate, the lower oxidation state vanadium oxides must first be oxidized to V_2O_5. This oxidation process can be represented by the following reaction:

$$V_2O_3 + O_2 = V_2O_5 \qquad (2)$$
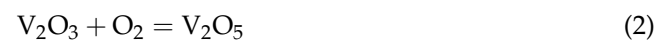
This reaction is thermodynamically possible with $\Delta G_o = -77.038$ kJ/mol at a temperature of 1600 °C and O_2 pressure of 101.3 kPa [35].

Authors [36–38] studied the effect of oxygen partial pressure and slag basicity on the vanadium oxidation state. The results suggest that the oxidation of V^{3+} in the solution state through reaction) is challenging. Similarly, V^{4+} can also be oxidized through this mechanism. To facilitate the evaporation of vanadium pentoxide from the liquid slag surface, it is necessary to oxidize the lower valent states of vanadium to V_2O_5 and transport it to the surface of the liquid slag. The main objective of the current study is to investigate the feasibility of removing vanadium in the form of oxide vapor from the liquid slag and subsequently condensing it for further use.

3. Experimental

3.1. Materials and Sample Preparation

For the experiments, the synthetic slag samples were prepared from pure oxides. $CaCO_3$ powder was calcined at 1273 K (1000 °C) in a muffle furnace for 8 h to release CO_2 gas from limestone decomposition. SiO_2 and V_2O_5 powders were heat-treated at

383 K (110 °C) for 5 h to remove any moisture. The wustite (FeO) was synthesized from stoichiometric amounts of Fe and Fe$_2$O$_3$ powders. The mixture was mixed in an agate mortar, placed into an iron crucible (purity 99.9%) with a tight iron lid, and kept at 1373 K (1100 °C) in an argon atmosphere for 24 h to reach equilibrium. The crucible was then air-cooled. The FeO produced was examined by XRD to confirm the absence of metallic iron and magnetite.

After mixing the chemicals in appropriate proportions, the slag was pre-melted in an induction furnace in an inert atmosphere in an iron crucible at 1673 K (1400 °C), sufficient to get homogeneous liquid slag. Then the crucible with a sample was fast-cooled without contact with air. The slag composition by XRF was found to be close to the fractions from the initially weighted amounts. No vanadium loss was detected.

For each slag composition, a series of experimental samples was prepared. This was carried out to check the influence of different treatment time sequences under oxygen and argon atmosphere. The prepared series of slag mixtures were stored in a desiccator until used.

The following slag compositions were used for the experiments (Table 1). This slag composition was already tested by authors previously [25] but the method used for the evaluation of the results was different. Moreover. In the current work, authors focused attention on the influence of basicity as well as studying the effect of atmospheres used for heat treatment.

Table 1. Synthetic slag compositions.

Sample Name	CaO/SiO$_2$ Ratio	CaO, wt.%	SiO$_2$, wt.%	FeO, wt.%	V$_2$O$_5$, wt.%
CSFV1	0.8	33.6	42.0	20.0	4.4
CSFV2	1.0	37.8	37.8	20.0	4.4
CSFV3	1.2	41.2	34.4	20.0	4.4
CSFV4	1.4	44.1	31.5	20.0	4.4

3.2. Experimental Set-Up

The experiments were performed using Single Hot Thermocouple Technique (SHTT) (Figure 5) custom built at TU Bergakademie Freiberg, Germany. SHTT is usually used for studying the crystallization and the development of time-temperature-transformation diagrams. As thin film experiments at SHTT have perfect conditions to study the evaporation process due to a very high surface-to-volume ratio, it was used for the current experiments to have both slag surfaces available for evaporation.
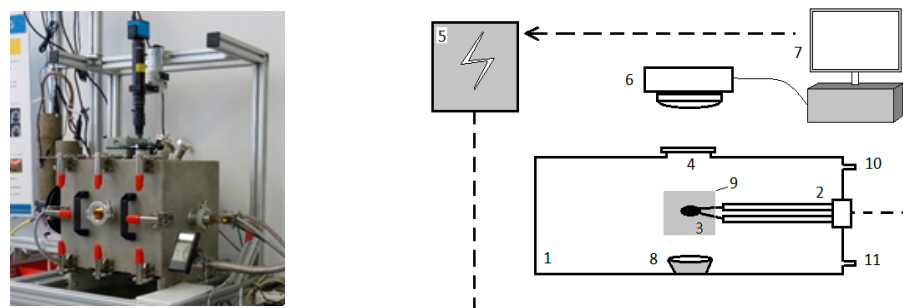

Figure 5. The experimental apparatus—Single Hot Thermocouple Technique (SHTT) [25] 1—vacuum chamber, 2—insert, 3—thermocouple, 4—sealed window, 5—electronic circuit, 6—CCD camera, 7—computer control, 8—lamp, 9—additional heating, 10—gas exit to pump, 11—gas inlet for air or Ar.

A thin film sample of slag weighing approximately 5 milligrams was held on a B-type loop thermocouple made of Pt-30 wt.% Rh/Pt-6 wt.% Rh wire with a diameter of 0.5 mm. The loop size was approximately 2.5 mm in outer diameter. The thermocouple was utilized both for heating the sample and measuring its temperature. The temperature was controlled by a temperature controller. The experiments were carried out within a temperature range of 1380 °C to 1420 °C.

The heat treatment procedures applied in this study consisted of two sequences. The first sequence involved heating the sample at a rate of 100 °C/min in an argon atmosphere to the target temperature, followed by a pre-treatment period of 35 min to establish thermal equilibrium. The sample was then air treated for varying durations (0, 1, 5, 20, 45, and 60 min) and then cooled down at a rate of 40 °C/min in argon. The second sequence was similar, with the exception that the sample was treated with argon instead of air for the same duration periods.

3.3. Samples Analysis

After the SHTT experiments, the samples were mounted and analyzed on a Scanning Electron Microscope (SEM) coupled with energy-dispersive X-ray spectroscopy (EDX). The used SEM was a Quanta 250 FEG manufactured by FEI, and the EDX analysis was performed using an Octane Plus silicon drift detector (SDD) from Ametek/EDAX. To determine the elemental composition of each slag sample, their polished and well-defined zone were analyzed using both EDX area analysis and elemental mapping. Elemental mapping was found to be more precise in terms of a relative measuring error and was therefore chosen for further evaluation. Unlike backscatter electron (BSE) images that have a limited gray-scale range, EDX mapping displays the true spatial distribution of each element based on the time the beam dwells on each point. The EDX mapping parameters were set to a mapping resolution of 512 × 400 points, 32 frames, and a dwell time of 1000 s. Bulk chemical analysis by XRF after the thin slag experiments was not possible due to the small size of the samples, so the average composition was determined with EDX. V_2O_5 content was calculated stoichiometrically by dividing vanadium content in the sample by a conversion factor of 0.56 (assuming that all vanadium is in the form of V_2O_5).

4. Results and Discussion

Figure 6 displays a cross-sectional view of the thin slag formed in the thermocouple loop. The convex shape of the slag film is due to the competing effect of wetting between the Pt-thermocouple and the slag's surface tension. Such a convex shape has the advantage of increasing the evaporative surface area exposed to the surrounding atmosphere.
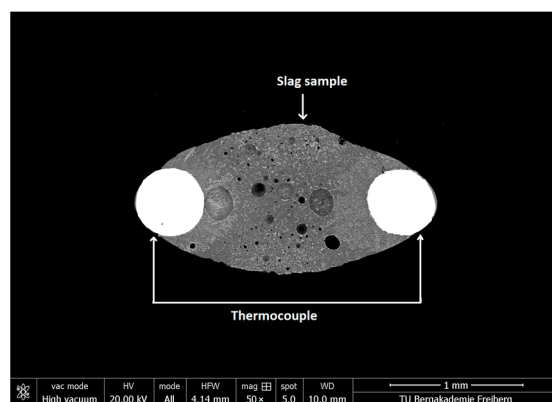

Figure 6. The cross-section of the slag film in the thermocouple loop.

In the previous thin-film slag studies conducted by the authors [28,29], simple spot analysis and line SEM-EDX analyses to determine the vanadium content in the slag sample were performed. This method involved analyzing 10 points on each sample and calculating

the average vanadium value. However, after the application of the mapping technique such analysis was found to underestimate the vanadium content in the slag. To address this issue, area mapping was employed, which confirmed the loss of vanadium from the sample, but to a much lesser extent. Figure 7 compares the average vanadium pentoxide content in the slag obtained through the previous method (a) with those obtained through area analysis (b) as a function of oxygen treatment time.
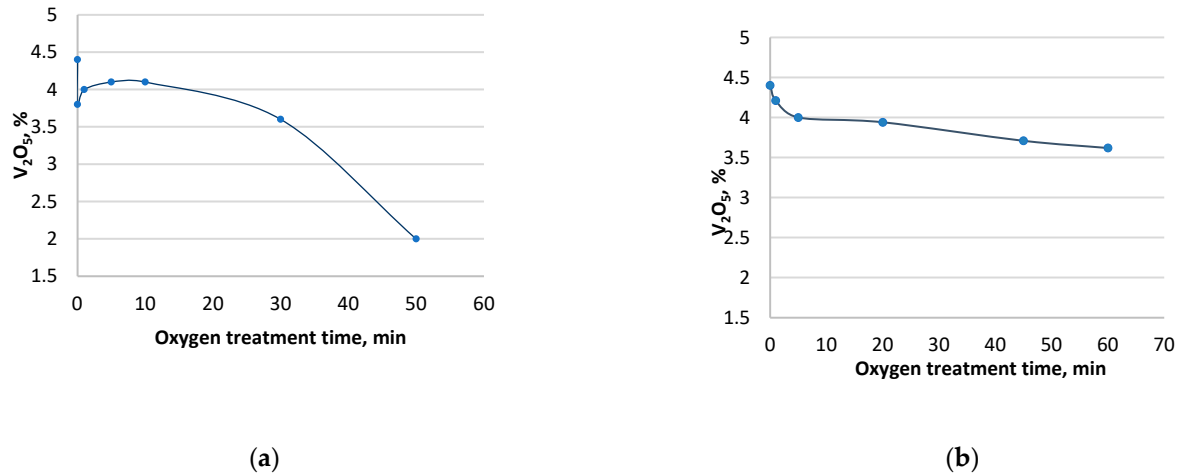

(**a**)

(**b**)

Figure 7. The average content of vanadium pentoxide as a function of oxygen treatment time was measured with spot analysis (**a**) [28] and with area mapping (**b**) in SEM EDX.

The investigation of four slag systems with varying binary basicities ($CaO/SiO_2 = 0.8$, 1.0, 1.2, 1.4) revealed that vanadium pentoxide evaporation rate as a function of air treatment time is higher at lower basicities of the slag (Figure 8). The vanadium pentoxide extraction rate for the slag with binary basicity of 0.8 was found to be 17.73%. In comparison, the basicities of 1.2 and 1.4 showed a vanadium pentoxide extraction rate of 10.45%. It is hypothesized that the evaporation of V is primarily controlled by diffusion through the slag mass.
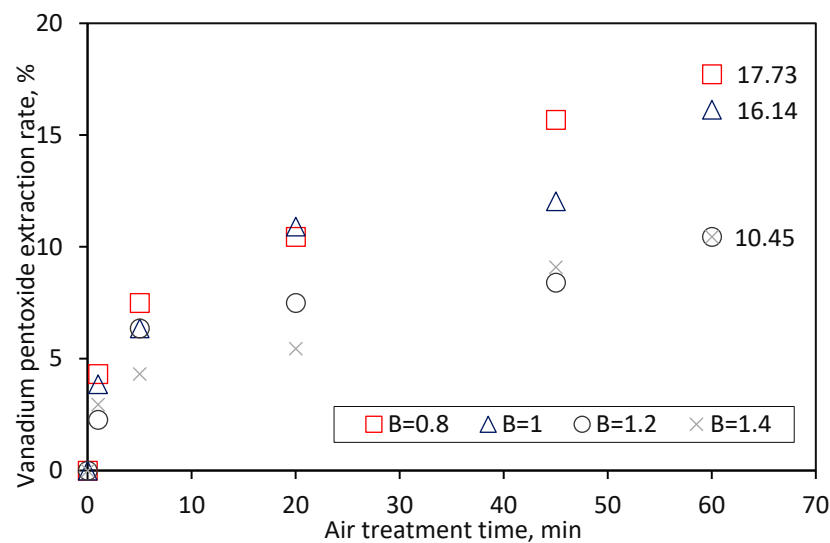

Figure 8. Effect of basicity on vanadium pentoxide evaporation rate as a function of air treatment time.

Calculation of viscosity (Figure 9a) for the initial samples was carried out with the use of the Iida model [39], given in tables by Mills [40]. Iida viscosity model considers the network structure of the slag using modified basicity index Bi^*:

$$\mu = A\mu_0 \exp\left(\frac{E}{Bi^*}\right), \ (\text{Pa} * \text{s})$$ (3)

where μ_0 is the viscosity of hypothetical network forming melt and Bi^* is a modified basicity index.

$$A = 1.745 - 1.962 \times 10^{-3}T + 7 \times 10^{-7}T^2$$ (4)

$$E = 11.11 - 3.65 \times 10^{-3}T$$ (5)

$$B_i^* = \frac{\sum(\alpha_i\%_i)_B}{\sum(\alpha_i\%_i)_A}$$ (6)

where A—acid oxides and B—basic oxides or fluorides.

$$\mu_0 = \sum_{i=1}^{n} \mu_{0i}X_i$$ (7)

and μ_{0i} values can be calculated using the expression:

$$\mu_{0i} = 1.8 \times 10^{-7}\frac{[M_i(T_m)_i]^{1/2}\exp(H_i/RT)}{(V_m)_i^{2/3}\exp[H_i/R(T_m)_i]}, \ (\text{Pa·s})$$ (8)

$$H_i = 5.1(T_m)_i^{1/2}$$ (9)

where M is the formula weight, V_m is the molar volume at the melting point T_m, R is the gas constant, X is the mole fraction, and i refers to the component.
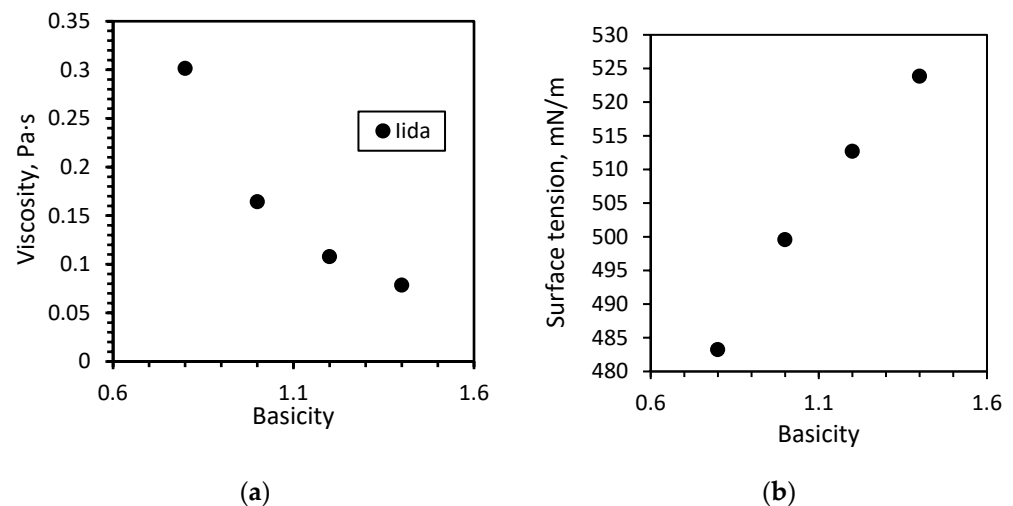

Figure 9. Viscosity (**a**) and surface tension (**b**) were calculated using the Iida model and method 2a in Mills tables [40].

The surface tension was calculated using a partial molar approach (Figure 9b) [40]:

$$\gamma = \Sigma X_1 \gamma_1 + X_2 \gamma_2 + X_3 \gamma_3 + \ldots$$ (10)

Despite the absence of V_2O_5 data in Mills' table, it was presumed that the vanadium present in the liquid existed in the form of V^{3+} or V^{4+} ions. The vanadium content was then

converted into V_2O_3. In the calculation of the optical basicity of the slag, it was postulated that V_2O_3 possessed similar characteristics to Cr_2O_3. This assumption was made based on the similar effect on viscosity [41,42] and surface tension of both chromium and vanadium oxides [43]. Analysis revealed a decrease in viscosity along with the basicity rise. At the same time, surface tension (Figure 9b) is slightly increasing with basicity. Therefore, the physical properties of liquid should generally favor the evaporation process. However, this contradicts our observations and indicates other phenomena affecting the evaporation of V_2O_5.

The most probable explanation of the inhibitory effect of basicity on the evaporation rate could be the binding of V_2O_5 with CaO. Wang et al. [27] studied the effect of CaO on V_2O_5 volatilization and reported that the addition of CaO reduced the activity of V_2O_5 and decreased its volatilization rate. The reason is that CaO and V_2O_5 form calcium vanadates—namely $CaO \cdot V_2O_5$, $2CaO \cdot V_2O_5$, and $3CaO \cdot V_2O_5$. These are relatively high melting point compounds (Figure 10). On the other hand, according to the FactSage calculations, the amount of liquid phase in the studied slag systems is also affected by the increase of basicity. At 1400 °C, the slag system with 44.1 wt.% CaO, 31.5 wt.% SiO_2, 20 wt.% FeO, 4.4 wt.% V_2O_5 and the binary basicity of 1.4 has 13.4% of solid fraction while other slags are completely liquid. As per the three-phase diagram for CaO-SiO$_2$-FeO normalized without V_2O_5 at 1400 °C (Figure 11), all four slags should be in a liquid state.
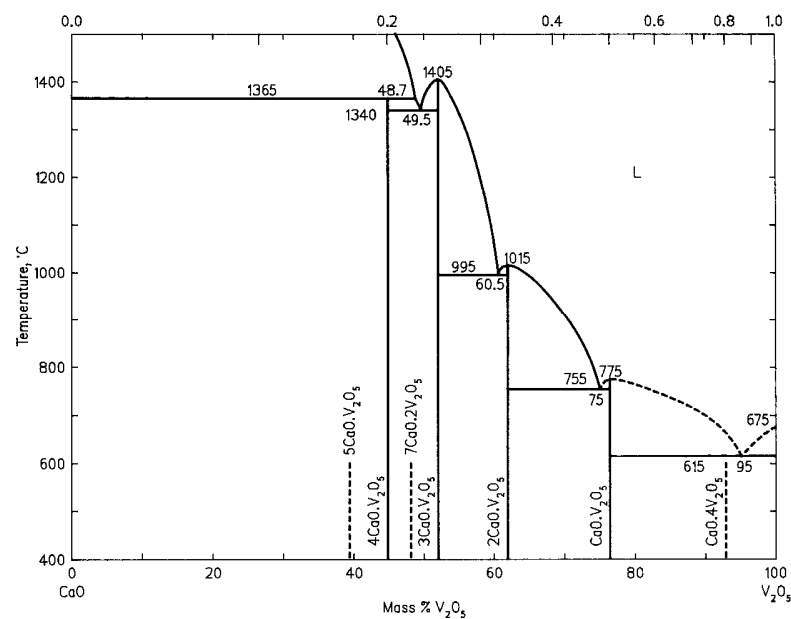

Figure 10. Phase diagram of CaO-V_2O_5 system [43].

Thus, it is expected that the evaporation rate of vanadium pentoxide would be significantly lower in samples with a higher basicity, as the fraction of the solid phase increases together with calcium vanadate formation.

Wang et al. [27] studied the effect of CaO on V_2O_5 volatilization and discovered that the addition of CaO reduced the activity of V_2O_5 and decreased its volatilization rate.

The slag sample with the binary basicity of 0.8 had homogeneous dendritic precipitations after 1 min air treatment. After 60 min only some dendritic precipitates were left on the sample's borders. The rest of the sample was constituted of an amorphous matrix (Figure 12). Spot analysis of the sample after 1 min treatment at the air conditions revealed a high concentration of V in the matrix, while dendrites had an elevated share of Fe.
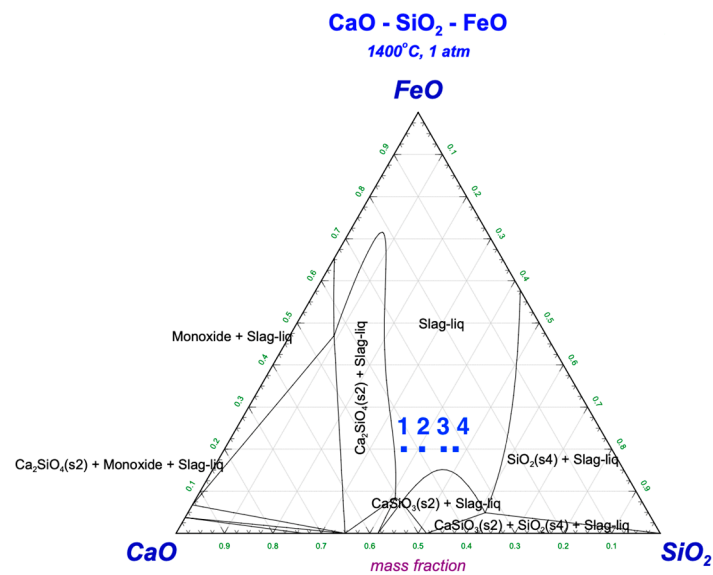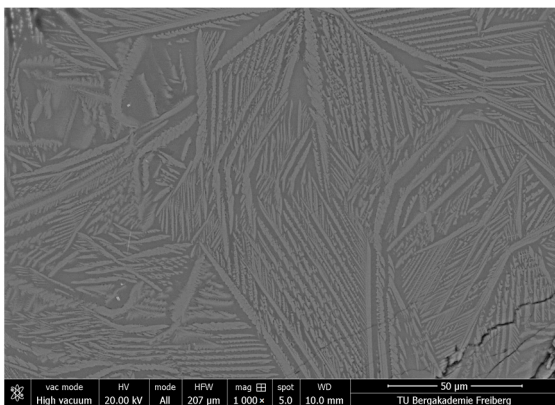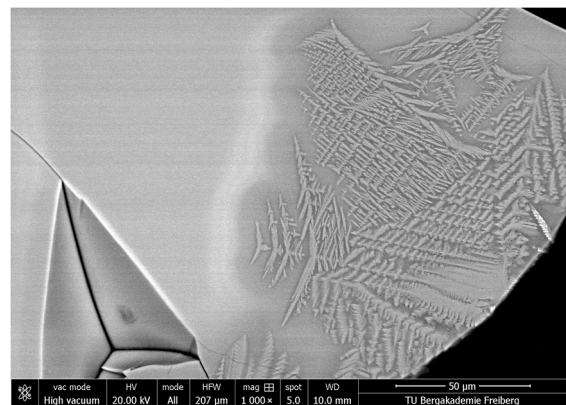
Figure 11. Phase diagram for CaO-SiO$_2$-FeO system and compositions of the samples with CaO/SiO$_2$ = 0.8 (point 1), 1.0 (point 2), 1.2 (point 3), and 1.4 (point 4) normalized without V$_2$O$_5$ at 1400 °C.

Figure 12. SEM micrographs of the slag sample 33.6% CaO—42.0% SiO$_2$—20% FeO—4.4% V$_2$O$_5$ (CaO/ SiO$_2$ = 0.8) at different air treatment time: (**a**) 1 min, (**b**) 60 min (*T* = 1400 °C).

The samples with the binary basicities of 1.0, 1.2, and 1.4 had similar behavior during air heat treatment. After 1 min slag had an amorphous matrix surrounded by iron oxide dendrites and V-rich oxides bound into calcium silicate Ca$_2$SiO$_4$ matrix (Figure 13). As can be seen from the figure, the size of the crystals was changing while increasing the treatment time. The crystal formations, in particular vanadium ferrites FeV$_2$O$_4$ and Fe$_2$VO$_4$, for CaO-SiO$_2$-FeO- V$_2$O$_5$ system were studied by Semykina et al. [44].

To assure that no vanadium from the slag was alloyed with the Pt-thermocouple during the SHTT experiments, the thermocouple cross-section was examined. The SEM/EDX analysis revealed no vanadium in the Pt phase (Figure 14).

During the experiments conducted under a pure argon atmosphere, a high amount of bubbles formation was detected (Figure 15). The bubbles are not colliding with other bubbles due to low interfacial tension and high viscosity. No loss of vanadium was detected by the SEM/EDX mapping.
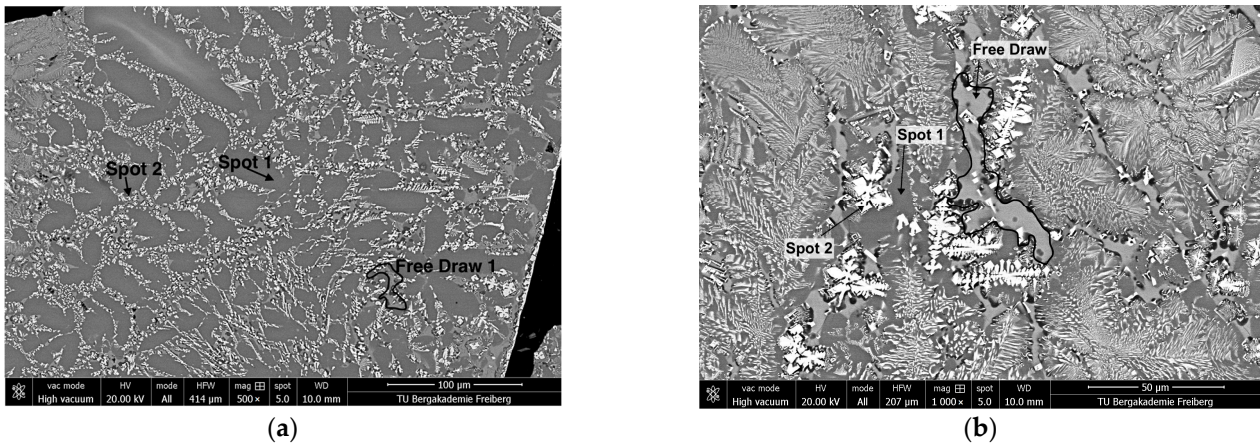
Figure 13. SEM micrographs of the slag sample 37.8% CaO—37.8% SiO$_2$—20% FeO—4.4% V$_2$O$_5$ at different air treatment times: (**a**) 1 min, (**b**) 60 min ($T = 1400\ ^\circ$C); Spot 1 (dark grey color)—wollastonite CaSiO$_3$, Spot 2 (white color)—iron oxides, Free Draw (light grey color)—V-rich oxides (possibly FeV$_2$O$_4$) and calcium silicate Ca$_2$SiO$_4$.
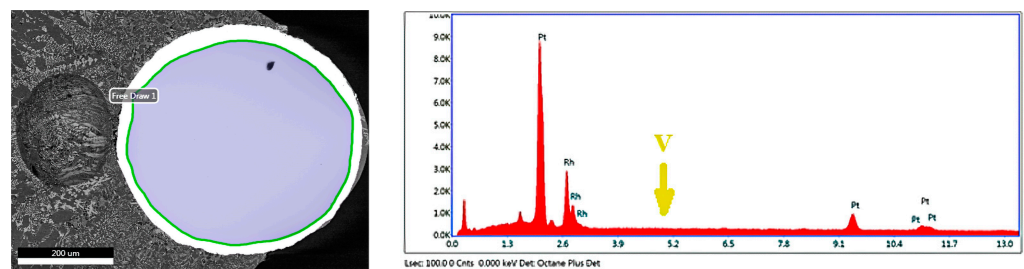

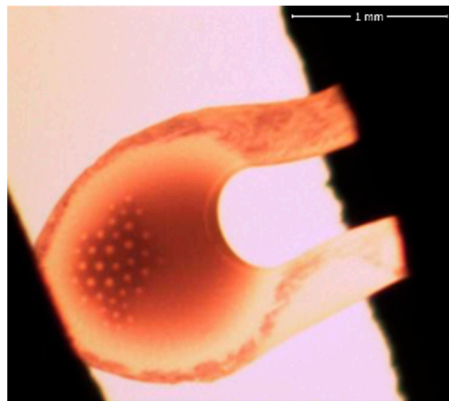**Figure 14.** Spectral analysis of Pt-thermocouple by SEM/EDX and its spectrum.

Figure 15. Molten slag inside the thermocouple during the SHTT experiment.

The atomic mass of different elements on Spot 1 indicated that vanadium existed in the form of spinel (FeV$_2$O$_4$) (Figures 16 and 17). SEM/EDX mapping of elements showed that the highest V content was in the inner surfaces of the bubbles. This indicates that in the absence of an oxygen atmosphere, vanadium pentoxide remains entrapped in the bubbles formed inside the slag.
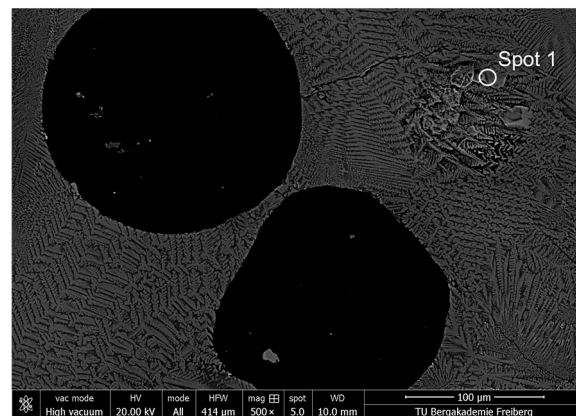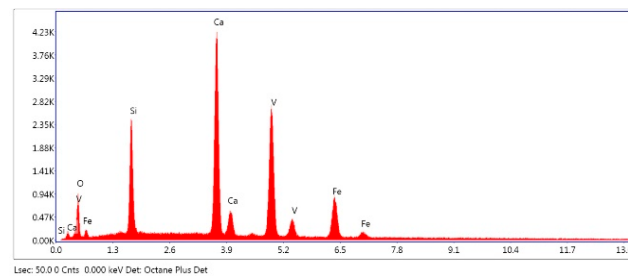
Figure 16. SEM micrograph of argon-treated slag sample.

Element	Weight%	Atomic%
O K	15.05	32.68
SiK	9.48	11.72
CaK	27.74	24.04
V K	31.22	21.29
FeK	16.51	10.27

Figure 17. SEM/EDX results of argon-treated slag sample.

Scientists have shown a keen interest in FeV_2O_4 due to the presence of various quantum mechanical phenomena, including successive structural phase transitions, orbital degree of freedom for both Fe^{2+} and V^{3+} ions, spin frustration while interacting between electromagnetism and lattice structure, and spin glass [45,46]. In the current study, FeV_2O_4 crystals were observed under an argon atmosphere during the formation of bubbles in the SHTT equipment. The other authors [44] have previously obtained similar results for V-bearing slags during experiments in a horizontal furnace under an argon atmosphere and oxygen partial pressures $P_{O_2} = 10^{-1} - 10^{-2}$ Pa. The obtained spinels could potentially be separated from the slag using magnetic separation.

5. Conclusions

During the experiments with thin films of vanadium-containing slags at 1380–1420 °C in argon and air atmospheres different phenomena of vanadium oxides behavior were observed. Under the air atmosphere vanadium oxides tend to evaporate from the slag. The maximum achieved evaporation was 17.73% after 1 h of air treatment. An increase in basicity lowers the evaporation rate due to the formation of calcium vanadates. Under the argon atmosphere, slag had a high number of bubbles entrapped. SEM/EDX results revealed FeV_2O_4 spinel formation which is valuable material as such and can be magnetically separated.

The obtained results can serve as the background for two ways of V-extraction and as a background for designing a new vanadium extraction technique on the plant practice. The synthetic slags from the present study were exposed only to the natural convection of air and argon. It is expected that targeted air or oxygen treatment should improve the oxidation and evaporation of vanadium. Additionally, results raise a concern about the potential health hazard of working with the molten vanadium-bearing slags associated with the inhalation of toxic V_2O_5 vapors.

References

1. Worldsteel Association Fact Sheet. Steel Industry Co-Products. Available online: https://worldsteel.org/wp-content/uploads/Fact-sheet-Steel-industry-co-products.pdf (accessed on 1 March 2023).
2. IARC Working Group on the Evaluation of Carcinogenic Risks to Humans. *Cobalt in Hard Metals and Cobalt Sulfate, Gallium Arsenide, Indium Phosphide, and Vanadium Pentoxide*; World Health Organization International Agency for Research on Cancer: Lyon, France; Geneva, Switzerland, 2006; ISBN 978-92-832-1286-7.
3. Bin Li, X.; Wei, C.; Deng, Z.G.; Li, M.T.; Li, C.X.; Xu, H.S. Acid Leaching of Vanadium from a Vanadium Residue. *Adv. Mater. Res.* **2011**, *402*, 243–248. [CrossRef]
4. Xiang, J.; Huang, Q.; Lv, X.; Bai, C. Extraction of vanadium from converter slag by two-step sulfuric acid leaching process. *J. Clean. Prod.* **2018**, *170*, 1089–1101. [CrossRef]
5. Zhang, G.-Q.; Zhang, T.-A.; Lü, G.-Z.; Zhang, Y.; Liu, Y.; Liu, Z.-L. Extraction of vanadium from vanadium slag by high pressure oxidative acid leaching. *Int. J. Miner. Met. Mater.* **2015**, *22*, 21–26. [CrossRef]
6. Aarabi-Karasgani, M.; Rashchi, F.; Mostoufi, N.; Vahidi, E. Leaching of vanadium from LD converter slag using sulfuric acid. *Hydrometallurgy* **2010**, *102*, 14–21. [CrossRef]
7. Zhang, X.; Fang, D.; Song, S.; Cheng, G.; Xue, X. Selective leaching of vanadium over iron from vanadium slag. *J. Hazard. Mater.* **2019**, *368*, 300–307. [CrossRef] [PubMed]
8. Li, H.-Y.; Wang, C.-J.; Yuan, Y.-H.; Guo, Y.; Diao, J.; Xie, B. Magnesiation roasting-acid leaching: A zero-discharge method for vanadium extraction from vanadium slag. *J. Clean. Prod.* **2020**, *260*, 121091. [CrossRef]
9. Chen, D.; Zhao, L.; Liu, Y.; Qi, T.; Wang, J.; Wang, L. A novel process for recovery of iron, titanium, and vanadium from titanomagnetite concentrates: NaOH molten salt roasting and water leaching processes. *J. Hazard. Mater.* **2013**, *244-245*, 588–595. [CrossRef]
10. Liu, B.; Meng, L.; Zheng, S.; Li, M.; Wang, S. A novel method to extract vanadium from high-grade vanadium slag: Non-salt roasting and alkaline leaching. *Physicochem. Probl. Miner. Process.* **2018**, *54*, 657–667.
11. Li, H.-Y.; Fang, H.-X.; Wang, K.; Zhou, W.; Yang, Z.; Yan, X.-M.; Ge, W.-S.; Li, Q.-W.; Xie, B. Asynchronous extraction of vanadium and chromium from vanadium slag by stepwise sodium roasting–water leaching. *Hydrometallurgy* **2015**, *156*, 124–135. [CrossRef]
12. Ye, G.; Burstrom, E.; Kuhn, M.; Piret, J. Reduction of steel-making slags for recovery of valuable metals and oxide materials. *Scand. J. Met.* **2003**, *32*, 7–14. [CrossRef]
13. Mirazimi, S.M.J.; Rashchi, F. Optimization of Bioleaching of a Vanadium Containing Slag Using RSM. In Proceedings of the 7th International Chemical Engineering Congress & Exihibition, Kish, Iran, 21–24 November 2011; p. 11.
14. Mahdavian, A.; Shafyei, A.; Alamdari, E.K.; Haghshenas, D.F. Recovery of vanadium from esfahan steel company steel slag; Optimizing of roasting and leaching parameters. *Int. J. Iron Steel Soc. Iran* **2006**, *3*, 17–21.
15. Jia, L.; Zhang, Y.; Tao, L.; Jing, H.; Bao, S. A methodology for assessing cleaner production in the vanadium extraction industry. *J. Clean. Prod.* **2014**, *84*, 598–605. [CrossRef]
16. Yuan, J.; Cao, Y.; Fan, G.; Du, H.; Dreisinger, D.; Han, G.; Li, M. Study on the Mechanisms for Vanadium Phases' Transformation of Vanadium Slag Non-Salt Roasting Process. In *Proceedings of the Rare Metal Technology 2020*; Azimi, G., Forsberg, K., Ouchi, T., Kim, H., Alam, S., Baba, A.A., Eds.; Springer International Publishing: Cham, Switzerland, 2020; pp. 235–242.
17. Hu, P.; Zhang, Y.; Liu, H.; Liu, T.; Li, S.; Zhang, R.; Guo, Z. High efficient vanadium extraction from vanadium slag using an enhanced acid leaching-coprecipitation process. *Sep. Purif. Technol.* **2023**, *304*, 122319. [CrossRef]
18. Ji, Y.; Shen, S.; Liu, J.; Yan, S.; Zhang, Z. Green and Efficient Process for Extracting Chromium from Vanadium Slag by an Innovative Three-Phase Roasting Reaction. *ACS Sustain. Chem. Eng.* **2017**, *5*, 6008–6015. [CrossRef]

19. Ling, H.; Malfliet, A.; Blanpain, B.; Guo, M. Evaporation of Antimony Trioxide from Antimony Slag by Nitrogen Injection in a Top-Submerged Lance Smelting Set-Up. In *Proceedings of the 12th International Symposium on High-Temperature Metallurgical Processing*; Peng, Z., Hwang, J.-Y., White, J.F., Downey, J.P., Gregurek, D., Zhao, B., Yücel, O., Keskinkilic, E., Jiang, T., Mahmoud, M.M., Eds.; Springer International Publishing: Cham, Switzerland, 2022; pp. 133–142.

20. Persson, M.; Seetharaman, S.; Seetharaman, S. Kinetic Studies of Fluoride Evaporation from Slags. *ISIJ Int.* **2007**, *47*, 1711–1717. [CrossRef]

21. Ju, J.-T.; Ji, G.-H.; Tang, C.-M.; An, J.-L. Fluoride Evaporation and Melting Characteristics of CaF_2 -CaO-Al_2O_3-MgO-Li_2 O- (TiO_2) Slag for Electroslag Remelting. *Steel Res. Int.* **2020**, *91*, 2000111. [CrossRef]

22. Shimizu, K.; Cramb, A. Fluoride Evaporation from CaF_2-SiO_2-CaO Slags and Mold Fluxes in Dry and Humid Atmospheres. *High Temp. Mater. Process.* **2003**, *22*, 237–246. [CrossRef]

23. Seetharaman, S.; Albertsson, G.J.; Scheller, P. Studies of Vaporization of Chromium from Thin Slag Films at Steelmaking Temperatures in Oxidizing Atmosphere. *Met. Mater. Trans. B* **2013**, *44*, 1280–1286. [CrossRef]

24. Cheremisina, E.; Schenk, J. Chromium Stability in Steel Slags. *Steel Res. Int.* **2017**, *88*, 1700206. [CrossRef]

25. Seetharaman, S.; Shyrokykh, T.; Schröder, C.; Scheller, P.R. Vaporization Studies from Slag Surfaces Using a Thin Film Technique. *Met. Mater. Trans. B* **2013**, *44*, 783–788. [CrossRef]

26. Shyrokykh, T.; Schröder, C.; Scheller, P.R.; Shatokha, V.; Seetharaman, S. Studies of High Temperature Surface Oxidation of FeO-CaO-SiO_2-V_2O_5 Slags with the Use of Single Hot Thermocouple Technique. *Metall. Mater. Trans. B* **2012**, *44*, 4.

27. Wang, W.X.; Xue, Z.L.; Song, S.Q.; Li, P.; Chen, Z.C.; Liu, R.N.; Wang, G.L. Research on High-Temperature Volatilization Characteristics of V_2O_5 during Direct Alloying of Smelting Vanadium Steel. *Adv. Mater. Res.* **2012**, *557–559*, 182–186. [CrossRef]

28. Shyrokykh, T.; Wei, X.; Seetharaman, S.; Volkova, O. Vaporization of Vanadium Pentoxide from CaO-SiO_2-VO_x Slags During Alumina Dissolution. *Met. Mater. Trans. A* **2021**, *52*, 1472–1483. [CrossRef]

29. Bergerud, A.J. Phase Stability and Transformations in Vanadium Oxide Nanocrystals. Ph.D. Thesis, University of California, Berkeley, CA, USA, 2016.

30. Yamaguchi, I.; Manabe, T.; Tsuchiya, T.; Nakajima, T.; Sohma, M.; Kumagai, T. Preparation and Characterization of Epitaxial VO_2 Films on Sapphire Using Postepitaxial Topotaxy Route via Epitaxial V_2O_3 Films. *Jpn. J. Appl. Phys.* **2008**, *47*, 1022–1027. [CrossRef]

31. *FactSage*, Version 7.2; Centre for Research in Computational Thermochemistry: Quebec, QC, Canada; GTT-Technologies: Herzogenrath, Germany.

32. Kubaschewski, O.; Alcock, C.B. *Metallurgical Thermochemistry*, 5th ed.; Metallurgy: Moscow, Russia, 1982.

33. Yang, Y.; Teng, L.; Seetharaman, S. Kinetic Studies on Evaporation of Liquid Vanadium Oxide, VO_x (Where x = 4 or 5). *Met. Mater. Trans. B* **2012**, *43*, 1684–1691. [CrossRef]

34. Wang, L.; Teng, L.; Chou, K.-C.; Seetharaman, S. Determination of Vanadium Valence State in CaO-MgO-Al_2O_3-SiO_2 System By High-Temperature Mass Spectrometry. *Met. Mater. Trans. B* **2013**, *44*, 948–953. [CrossRef]

35. *HSC Chemistry*, Version 9.0; Chemistry Software: Houston, TX, USA: Houston, TX, USA.

36. Wang, H.; Wang, L.; Seetharaman, S. Determination of Vanadium Oxidation States in CaO-MgO-Al_2O_3-SiO_2-VO_x System by K Edge XANES Method. *Steel Res. Int.* **2015**, *87*, 199–209. [CrossRef]

37. Mittelstadt, R.; Schwerdtfeger, K. The dependence of the oxidation state of vanadium on the oxygen pressure in melts of VO_x, Na_2O-VO_x, and CaO-SiO_2-VO_x. *Met. Trans. B* **1990**, *21*, 111–120. [CrossRef]

38. Farah, H.; Brungs, M. Oxidation-reduction equilibria of vanadium in CaO-SiO_2, CaO-Al_2O_3-SiO_2 and CaO-MgO-SiO_2 melts. *J. Mater. Sci.* **2003**, *38*, 1885–1894. [CrossRef]

39. Iida, T.; Sakai, H.; Kita, Y.; Shigeno, K. An Equation for Accurate Prediction of the Viscosities of Blast Furnace Type Slags from Chemical Composition. *ISIJ Int.* **2000**, *40*, S110–S114. [CrossRef]

40. Mills, K. Ken Mills–Slag Modelling. Available online: https://www.pyrometallurgy.co.za/KenMills/ (accessed on 26 July 2020).

41. Wang, Z.; Bai, J.; Kong, L.; Wen, X.; Li, X.; Bai, Z.; Li, W.; Shi, Y. Viscosity of coal ash slag containing vanadium and nickel. *Fuel Process. Technol.* **2014**, *136*, 25–33. [CrossRef]

42. Wu, T.; Zhang, Y.; Yuan, F.; An, Z. Effects of the Cr_2O_3 Content on the Viscosity of CaO-SiO_2-10 Pct Al_2O_3-Cr_2O_3 Quaternary Slag. *Met. Mater. Trans. B* **2018**, *49*, 1719–1731. [CrossRef]

43. Mills, K. *Slag Atlas*, 2nd ed.; VDEh: Düsseldorf, Germany, 1995.

44. Semykina, A.; Dzhebian, I.; Shatokha, V. On the Formation of Vanadium Ferrites in CaO-SiO_2-FeO-V_2O_5 Slags. *Steel Res. Int.* **2012**, *83*, 1129–1134. [CrossRef]

45. Katsufuji, T.; Suzuki, T.; Takei, H.; Shingu, M.; Kato, K.; Osaka, K.; Takata, M.; Sagayama, H.; Arima, T.-H. Structural and Magnetic Properties of Spinel FeV_2O_4 with Two Ions Having Orbital Degrees of Freedom. *J. Phys. Soc. Jpn.* **2008**, *77*, 053708. [CrossRef]

46. Myoung, B.R.; Kim, S.J.; Lim, J.T.; Kouh, T.; Kim, C.S. Microscopic evidence of magnetic and structure phase transition in multiferroic spinel FeV_2O_4. *AIP Adv.* **2017**, *7*, 055828. [CrossRef]